GI_Forum 2022, Issue 1
Page: 98 - 106
Short Paper
Corresponding Author:
francesco.collivignarelli@stud.sbg.ac.at
DOI: 10.1553/giscience2022_01_s98

Enhanced Surface Water Mapping: An Integrated Solution for the Humanitarian Sector

Francesco Collivignarelli[1] and Lorenz Wendt[1]
[1]Paris Lodron University of Salzburg, Austria

Abstract

Remote sensing and geographic information technologies are widely used in various aspects of the humanitarian sector's activities. In the surface water mapping domain, Earth Observation plays a central role, enabling action at the level of disaster response as well as in preventive risk analysis. Most methodologies, however, rely on optical image analysis techniques that are not operational in cloudy conditions, that typically occur during the rainy season. In this article, we present a methodology that exploits SAR data exclusively. Being acquired in the microwave spectrum, SAR can operate irrespective of the weather and time of day. As a use case, we demonstrate the possible intersection of surface water layers with population and VGI data, which can provide enhanced information concerning displaced people and accessibility. The study area is the administrative unit level 3 of Pibor, South Sudan, which is reported to be particularly challenging in terms of logistics as well as for its environmental conditions. The results cover a multi-temporal dataset from 2017 to 2021, and a cross-validation is provided for a selected date showing an overall accuracy of 88.74% for the relevant surface water layer.

Keywords:

surface water mapping, synthetic aperture radar (SAR), humanitarian sector, displaced people, accessibility

1 Introduction

The use of GeoInformation (GI) and Earth Observation (EO) in the context of crises and emergencies exploits well-established procedures (Lang, Schoepfer, Zeil, & Riedler, 2017).

Remote sensing contributes in various aspects of humanitarian work, such as supporting the mapping and monitoring of refugee camps. It can also help to exploit environmental conditions, for example in optimizing water supply (Füreder, Tiede, Lüthje, & Lang, 2014; Kemper & Heinzel, 2014; Kranz et al., 2010; Lang, Tiede, Hölbling, Füreder, & Zeil, 2010).

When providing assistance, humanitarian organizations need up-to-date, trustworthy information regarding the situation on the ground and the environmental context (Lang et al., 2017). The requirement for accurate maps concerns all aid provision stages, from mission planning in an emergency to long-term care and maintenance, including assessing the

availability of natural resources such as ground and surface water, and estimating the immediate environment's nutritional capacity.

Flooding is a serious issue for South Sudan, where thousands of people get displaced (i.e., are forced to leave their homes) during strong floods. Such situations are linked to huge organizational difficulties in providing urgently needed aid (MSF, 2021). Due to their geographic setting, some areas have limited supply routes, and these may be inaccessible for several months of the year. In some cases, as in Pibor county, flooding can be so severe that even the airstrips become unusable, resulting in increases in travel time and transportation costs.

In this article, we present a surface water mapping methodology which relies exclusively on free-of-charge Sentinel-1 Copernicus (ESA, 1998) Synthetic Aperture Radar (SAR) data, to overcome the frequent cloud cover typical of the rainy season. The results are intersected with a demography dataset from WorldPop (University of Southampton, 2013) and VGI (OpenStreetMap foundation, 2004) to demonstrate the possibility of integrating a water detection pipeline in the context of humanitarian activities. The accuracy of gridded population datasets is currently debated, with few studies having been carried out for urban areas (Bai, Wang, Wang, Gao, & Sun, 2018; Thomson, Gaughan, et al., 2021; Thomson, Leasure, Bird, Tzavidis, & Tatem, 2021). The main aim is to deliver high-accuracy surface water maps. Intersecting these with population data provides a proxy of the size of the population involved in a single event. The results are presented for the administrative unit level 3 of Pibor, South Sudan.

2 Current status

In the domain of surface water mapping using remote sensing, with particular reference to high-resolution and free-of-charge data, various approaches have been proposed exploiting optical techniques (Acharya, Lee, Yang, & Lee, 2016; Du et al., 2016; Fan, Liu, Wu, & Zhao, 2020; Feyisa, Meilby, Fensholt, & Proud, 2014), SAR (Bioresita, Puissant, Stumpf, & Malet, 2018; Gulácsi & Kovács, 2020; Liang & Liu, 2020; Kel N. Markert et al., 2020), or both techniques (Hong, Jang, Kim, & Sohn, 2015; Irwin, Beaulne, Braun, & Fotopoulos, 2017; Kel N Markert, Chishtie, Anderson, Saah, & Griffin, 2018).

Concerning the use of SAR data, some methodologies are well-established. Common approaches aim to find an optimal threshold for backscatter to distinguish water from land, starting from the ordinary intensity thresholding (Otsu, 1979). These methods can be used irrespective of the weather and time of day. Global approaches (Cao, Zhang, Wang, & Zhang, 2019; Kel N. Markert et al., 2020; Uddin, Matin, & Meyer, 2019) on the other hand struggle with the conditions found in South Sudan, especially in terms of land-cover types and their shares, which affect full-image statistics. In fact, the seasonal trend of floods in South Sudan does not allow effective sampling of water pixels, as they are limited in some parts of the year and predominant in others.

Other methodologies using SAR combine change detection and thresholding (Long, Fatoyinbo, & Policelli, 2014; United Nations, 2020). These involve the selection of a reference

(pre-flood) image, which is time-consuming and not suitable when a fast response is needed. In addition, it is difficult to distinguish between permanent water and slow, persistent flooding, as the method is based on the detection of *abrupt* changes, resulting in an inaccurate delineation of the total extent of surface water at a given time.

The methodologies and solutions outlined above, therefore, do not fulfil the requirements for effective humanitarian action in the study area. Relying on SAR on-demand acquisitions can reduce timeliness and increase costs, and the use of optical imagery hampers operationality in certain weather conditions. When free-of-charge, systematically acquired data is used, the resolution is often not satisfactory, and change detection is not a viable option. In addition, the existing studies are all tuned for specific areas of interest, none of which feature the environmental conditions present in Pibor.

3 Methodology

To implement a robust surface water mapping solution, we exploit remote sensing (SAR) and freely available land-cover data. The resulting layers are then intersected with demography layers. All these data sources are processed, harmonized, and merged using JavaScript applications for a popular geospatial processing and visualization tool, Google Earth Engine (Google LLC, 2010). Figure 1 shows the general workflow.

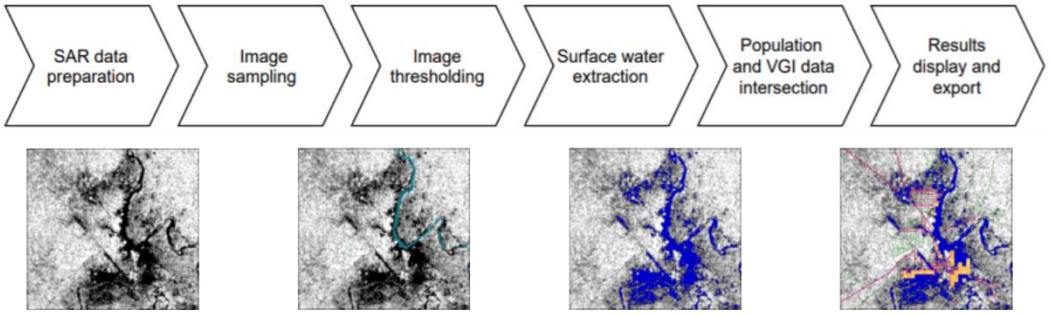

Figure 1: General workflow

3.1 Detailed workflow

SAR data preparation: the relevant Sentinel-1 SAR acquisition is selected according to date and area of interest. Then, it is radiometrically slope-corrected (Vollrath, Mullissa, & Reiche, 2020) and noise-filtered using Gamma MAP (Lopes, Nezry, Touzi, & Laur, 1993).

Image sampling: the pixels of the VV channel falling within a specific area delineated by an external land-cover class (ESRI, 2020) are selected. A histogram is computed using these samples.

Image thresholding: a threshold separating water from land is determined by iteratively evaluating the histogram retrieved in the previous step, using an adaptive method. This threshold

maximizes the inter-class variance (Otsu, 1979) and relies on the relative minima between two peaks of a bimodal distribution. A bimodality test is performed a-posteriori using normalized between-class variance (Demirkaya & H. Asyali, 2004).

Surface water extraction: the threshold is used on the whole image, so that any pixel that is associated with a backscatter value lower than its value is considered water.

Population and VGI data intersection: resulting surface water layers are overlaid with WorldPop and road features from OpenStreetMap. The surface water map is used as a mask for WorldPop, and all the road segments intersecting flooded pixels are selected and highlighted. The masked population layer is summarized to give a final estimate of the number of people living in flooded areas, who become displaced.

Results display and export: all the data generated is displayed in the Google Earth Engine canvas. In addition, statistics about population appear on the console to give a first-glance estimation of the number of displaced people. Full surface water maps and the masked population layer are optionally added to the task queue, enabling them to be downloaded for offline use.

An overview of a specific application of the workflow, where the results extracted for 30.09.2020 are visible, is shown in Figure 2.

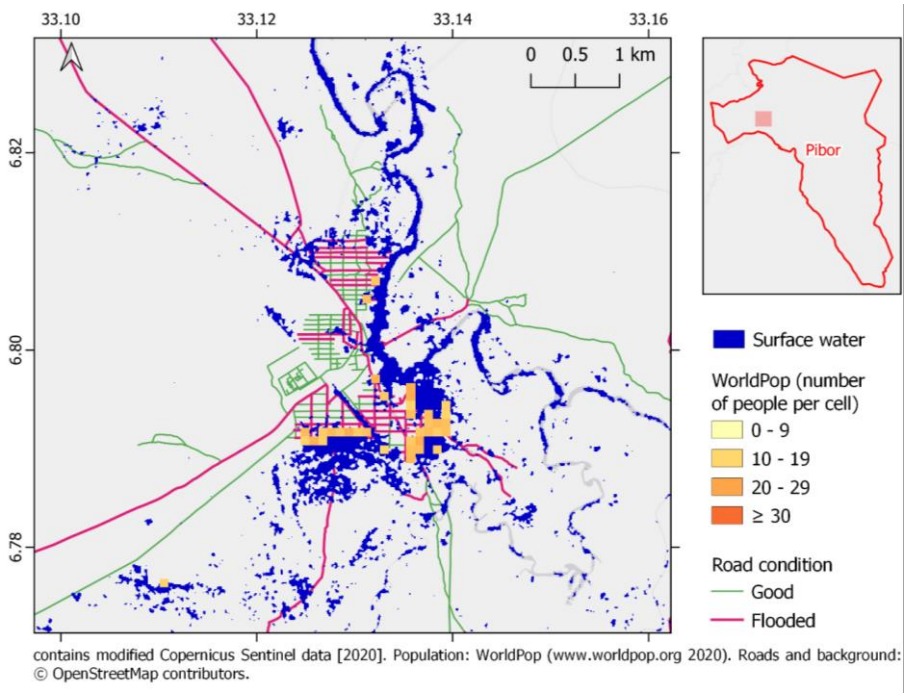

Figure 2: Results for 30.09.2020.

4 Results

Applying the methodology on all images in the Sentinel-1 archive from 2017 to 2021 over Pibor (78 acquisitions), it is possible to estimate the number of people displaced by flooding. These figures are summarized in the bar chart in Figure 3.

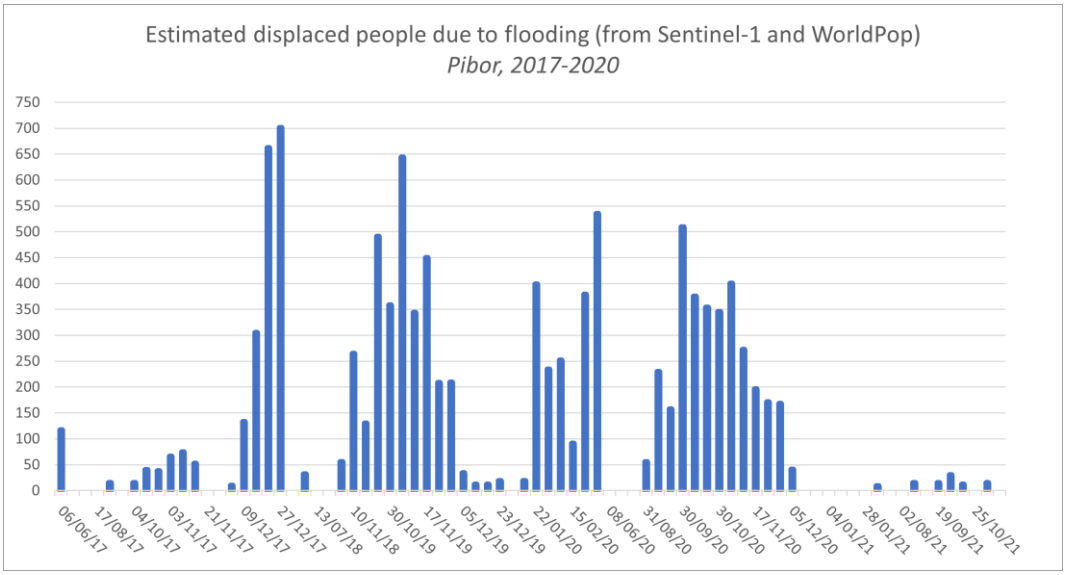

Figure 3: Estimated number of people displaced in Pibor due to flooding (2017–2021).

In quantitative terms, the results confirm how the study area has been affected by flooding events in recent years. For 2019 and 2020 in particular, a large number of surface water maps were generated with associated indications of high numbers of people involved. However, the date for which the largest number of people were affected appears to belong to 2017. In this year, on 27.12.2017, a total of 701 people were estimated to be living in flooded areas. As the accuracy of WorldPop is currently unknown, the number of displaced people has to be taken as a proxy, not as a precise statistic. However, this does not affect the effectiveness of precise surface water mapping in the humanitarian action context; the proxy can be taken as valid until such time as more accurate population layers become available. Full maps are plotted on the Google Earth Engine canvas and are available for download. In addition, the impact of the flooding event on roads is also shown. Due to the lack of ground recording data, for the surface water maps where simultaneous optical data exists cross-validation is carried out. A validation set is presented in Section 5.

5 Accuracy

Ground truth is frequently lacking for locations targeted by humanitarian action (Lang et al., 2015). However, sources of remote sensing data can serve for accuracy assessment. An optical cloud-free Sentinel-2 acquisition exists for 27.12.2017. The surface water map from the same date is cross-validated against NDVI (Pearson & Miller, 1972), by means of random sampling (Olofsson et al., 2014) over water and land classes. NDVI instead of a more accurate NDWI (Gao, 1996) was chosen because its spectral bands allow the generation of images at the same (10m) resolution as the Sentinel-1 SAR data, on which the methodology is based. A validation set and the relevant product can be seen in Figure 4.

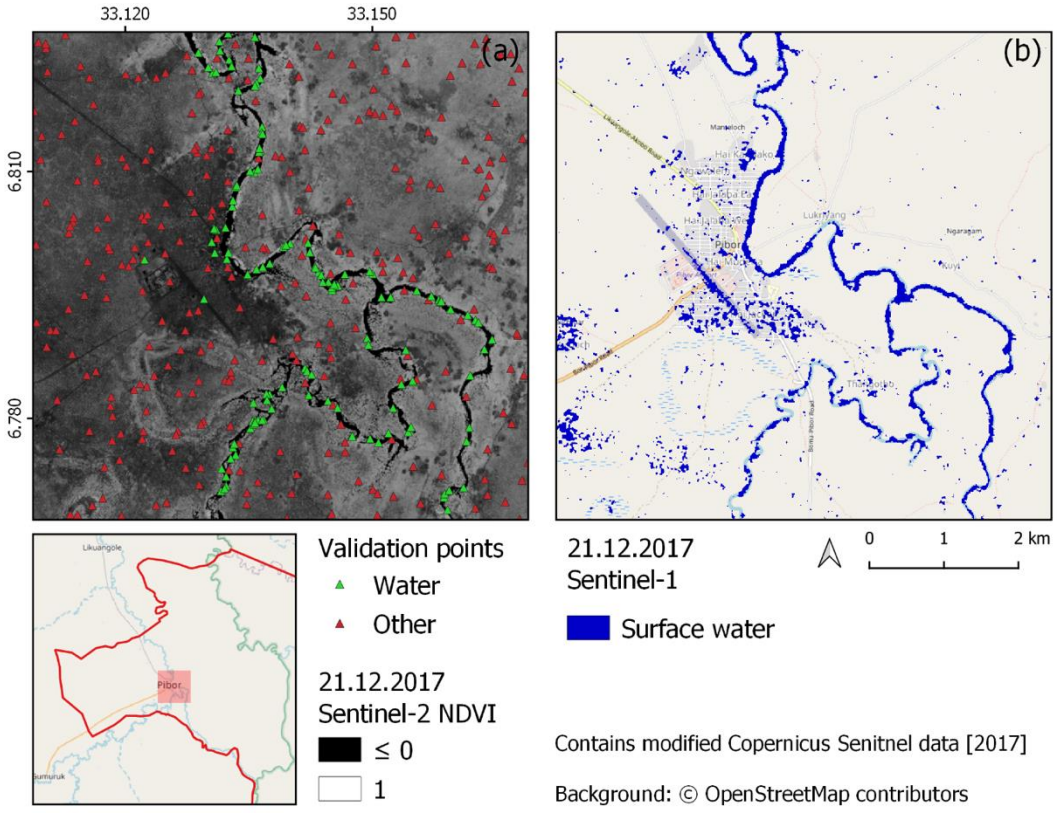

Figure 4: Validation set overlaid on NDVI data and relevant validated surface water map.

A confusion matrix is then computed by means of point sampling on the two layers. This is summarized in Table1 and shows an overall accuracy of 88.74%.

Table 1: Confusion matrix for 21.12.2017.

		Predicted class		Accuracy
		Water	Other	
Actual class	Water	110	13	89.43%
	Other	38	292	88.48%
		Overall:		88.74%

6 Conclusion and Outlook

This article highlights the effectiveness of using remote sensing data acquired in the microwave spectrum for the extraction of surface water maps, particularly in Pibor, South Sudan. The methodology proposed using Sentinel-1 data is designed to operate independently of weather conditions, enabling its use during the rainy season in tropical areas, when and where flood events are more likely to occur.

The 10 m Sentinel-1 resolution, combined with the large size of the swath, allows the targeting of large-scale events, which are the main objectives of humanitarian actors in the first stages of disaster response and action organization.

The set of layers generated demonstrate multi-year applicability and satisfactory robustness. More investigation regarding accuracy would be desirable, however; accuracy from the first assessment is promising. Using current data, cross-validation is possible for a few dates where matching optical acquisitions are available; one example is reported above.

Concerning the methodology itself, future expansions may concern downstream filtering after the classification step, as the maps sometimes appear to be affected by residual noise. These steps, however, are to be considered with great caution, to avoid missing the advantage offered by the excellent resolution of the data used.

The applications developed offer a useful tool to support the work of NGOs such as Médecins Sans Frontières (MSF). Their public release is a starting point for the refinement and further expansion of the methodology. One refinement could be the consideration of accessibility to places, or estimating the number of displaced people within a buffer rather than using simple intersection.

In conclusion, this research proposes an enhanced and user-friendly surface water mapping solution ready for further studies and product generation. The solution can bring current benefit and be of support and inspiration for the implementation of information delivery systems in the context of humanitarian action more widely.

Acknowledgements

This work was supported by the Austrian Federal Ministry for Digital and Economic Affairs, the National Foundation for Research, Technology and Development, the Christian Doppler Research Association (CDG), and Médecins Sans Frontières (MSF) Austria.

References

Acharya, T. D., Lee, D. H., Yang, I. T., & Lee, J. K. (2016). Identification of water bodies in a Landsat 8 OLI image using a J48 decision tree. *Sensors, 16*(7), 1075.

Bai, Z., Wang, J., Wang, M., Gao, M., & Sun, J. (2018). Accuracy assessment of multi-source gridded population distribution datasets in China. *Sustainability, 10*(5), 1363.

Bioresita, F., Puissant, A., Stumpf, A., & Malet, J.-P. (2018). A Method for Automatic and Rapid Mapping of Water Surfaces from Sentinel-1 Imagery. *Remote Sensing, 10*(2). doi:10.3390/rs10020217

Cao, H., Zhang, H., Wang, C., & Zhang, B. (2019). Operational Flood Detection Using Sentinel-1 SAR Data over Large Areas. *Water, 11*(4). doi:10.3390/w11040786

Demirkaya, O., & H. Asyali, M. (2004). Determination of image bimodality thresholds for different intensity distributions. *Signal Processing: Image Communication, 19*(6), 507-516. doi:10.1016/j.image.2004.04.002

Du, Y., Zhang, Y., Ling, F., Wang, Q., Li, W., & Li, X. (2016). Water bodies' mapping from Sentinel-2 imagery with modified normalized difference water index at 10-m spatial resolution produced by sharpening the SWIR band. *Remote Sensing, 8*(4), 354.

ESA. (1998). The Copernicus programme. Retrieved from https://www.esa.int/Applications/Observing_the_Earth/Copernicus

ESRI. (2020). ESRI 10-Meter Land Cover. Retrieved from https://livingatlas.arcgis.com/landcover/

Fan, X., Liu, Y., Wu, G., & Zhao, X. (2020). Compositing the Minimum NDVI for Daily Water Surface Mapping. *Remote Sensing, 12*(4). doi:10.3390/rs12040700

Feyisa, G. L., Meilby, H., Fensholt, R., & Proud, S. R. (2014). Automated Water Extraction Index: A new technique for surface water mapping using Landsat imagery. *Remote Sensing of Environment, 140*, 23-35.

Füreder, P., Tiede, D., Lüthje, F., & Lang, S. (2014). Object-based dwelling extraction in refugee/IDP camps–challenges in an operational mode. *South-Eastern European Journal of Earth Observation and Geomatics, 3*(2S), 539-544.

Gao, B.-C. (1996). NDWI—A normalized difference water index for remote sensing of vegetation liquid water from space. *Remote Sensing of Environment, 58*(3), 257-266.

Google LLC. (2010). Google Earth Engine. Retrieved from https://earthengine.google.com

Gulácsi, A., & Kovács, F. (2020). Sentinel-1-Imagery-Based High-Resolution Water Cover Detection on Wetlands, Aided by Google Earth Engine. *Remote Sensing, 12*(10). doi:10.3390/rs12101614

Hong, S., Jang, H., Kim, N., & Sohn, H. G. (2015). Water area extraction using RADARSAT SAR imagery combined with Landsat imagery and terrain information. *Sensors (Basel), 15*(3), 6652-6667. doi:10.3390/s150306652

Irwin, K., Beaulne, D., Braun, A., & Fotopoulos, G. (2017). Fusion of SAR, optical imagery and airborne LiDAR for surface water detection. *Remote Sensing, 9*(9), 890.

Kemper, T., & Heinzel, J. (2014). 10 Mapping and Monitoring of Refugees and Internally Displaced People Using EO Data. *Global urban monitoring and assessment through earth observation*, 195.

Kranz, O., Zeug, G., Tiede, D., Clandillon, S., Bruckert, D., Kemper, T., . . . Caspard, M. (2010). Monitoring refugee/IDP camps to support international relief action.

Lang, S., Füreder, P., Kranz, O., Card, B., Roberts, S., & Papp, A. (2015). Humanitarian emergencies: causes, traits and impacts as observed by remote sensing. In *Remote sensing of water resources, disasters, and urban studies* (pp. 483-512): CRC Press.

Lang, S., Schoepfer, E., Zeil, P., & Riedler, B. (2017). Earth Observation for Humanitarian Assistance. *GI_Forum, 1*, 157-165. doi:10.1553/giscience2017_01_s157

Lang, S., Tiede, D., Hölbling, D., Füreder, P., & Zeil, P. (2010). Earth observation (EO)-based ex post assessment of internally displaced person (IDP) camp evolution and population dynamics in Zam Zam, Darfur. *International Journal of Remote Sensing, 31*(21), 5709-5731.

Liang, J., & Liu, D. (2020). A local thresholding approach to flood water delineation using Sentinel-1 SAR imagery. *ISPRS Journal of Photogrammetry and Remote Sensing, 159*, 53-62. doi:10.1016/j.isprsjprs.2019.10.017

Long, S., Fatoyinbo, T. E., & Policelli, F. (2014). Flood extent mapping for Namibia using change detection and thresholding with SAR. *Environmental Research Letters, 9*(3), 035002.

Lopes, A., Nezry, E., Touzi, R., & Laur, H. (1993). Structure detection and statistical adaptive speckle filtering in SAR images. *International Journal of Remote Sensing, 14*(9), 1735-1758. doi:10.1080/01431169308953999

Markert, K. N., Chishtie, F., Anderson, E. R., Saah, D., & Griffin, R. E. (2018). On the merging of optical and SAR satellite imagery for surface water mapping applications. *Results in Physics, 9*, 275-277.

Markert, K. N., Markert, A. M., Mayer, T., Nauman, C., Haag, A., Poortinga, A., . . . Saah, D. (2020). Comparing Sentinel-1 Surface Water Mapping Algorithms and Radiometric Terrain Correction Processing in Southeast Asia Utilizing Google Earth Engine. *Remote Sensing, 12*(15). doi:10.3390/rs12152469

MSF. (2021). Third year of severe floods leaves nearly 800,000 people struggling. Retrieved from https://www.msf.org/third-year-floods-leaves-people-struggling-south-sudan

Olofsson, P., Foody, G. M., Herold, M., Stehman, S. V., Woodcock, C. E., & Wulder, M. A. (2014). Good practices for estimating area and assessing accuracy of land change. *Remote Sensing of Environment, 148*, 42-57. doi:https://doi.org/10.1016/j.rse.2014.02.015

OpenStreetMap foundation. (2004). OpenStreetMap. Retrieved from https://www.openstreetmap.org/

Otsu, N. (1979). A Threshold Selection Method from Gray-Level Histograms. *IEEE Transactions on Systems, Man, and Cybernetics, 9*(1), 62-66. doi:10.1109/TSMC.1979.4310076

Pearson, R. L., & Miller, L. D. (1972). Remote mapping of standing crop biomass for estimation of the productivity of the shortgrass prairie. *Remote sensing of environment, VIII*, 1355.

Thomson, D. R., Gaughan, A. E., Stevens, F. R., Yetman, G., Elias, P., & Chen, R. (2021). Evaluating the accuracy of gridded population estimates in slums: A case study in Nigeria and Kenya. *Urban Science, 5*(2), 48.

Thomson, D. R., Leasure, D. R., Bird, T., Tzavidis, N., & Tatem, A. J. (2021). How accurate are WorldPop-Global-Unconstrained gridded population data at the cell-level?: A simulation analysis in urban Namibia.

Uddin, Matin, & Meyer. (2019). Operational Flood Mapping Using Multi-Temporal Sentinel-1 SAR Images: A Case Study from Bangladesh. *Remote Sensing, 11*(13). doi:10.3390/rs11131581

United Nations. (2020). Step-by-Step: Recommended Practice: Flood Mapping and Damage Assessment Using Sentinel-1 SAR Data in Google Earth Engine. Retrieved from https://www.un-spider.org/advisory-support/recommended-practices/recommended-practice-google-earth-engine-flood-mapping/step-by-step

University of Southampton. (2013). WorldPop. Retrieved from https://www.worldpop.org/

Vollrath, A., Mullissa, A., & Reiche, J. (2020). Angular-Based Radiometric Slope Correction for Sentinel-1 on Google Earth Engine. *Remote Sensing, 12*(11). doi:10.3390/rs12111867